Experimental Validation of Optical Wireless Receiver using Solar Panel with Bandwidth Enhancement Circuit

Rahul [1], Abhijit Mitra [1], Anand Srivastava [1] , Vivek Ashok Bohara [1] and Deepak Solanki [2]
[1]Department of Electronics & Communication Engineering, IIIT-Delhi, New Delhi, India, 110020
{rahuli, abhijit, anand, vivek.b}@iiitd.ac.in
[2]Velmenni R&D, New Delhi, India, 110020
deepak@velmenni.com

***Abstract*—This paper presents a bandwidth enhancement circuit that enhances the 3 dB bandwidth of an off-the-shelf solar panel based receiver system for optical wireless communication. Experiment results show enhancement of the 3 dB bandwidth from 163 kHz to 1.62 MHz. A data rate of 1.5 Mbps is achieved with the OOK modulation scheme over the VLC link of 1 m. To the best of our knowledge, this is the highest data rate using solar panel as a receiver with OOK modulation. Low-cost, larger receiving area, ease of integration with other devices make the proposed system an environment-friendly and energy-efficient solution for optical wireless communication.**

***Index Terms*—Visible Light Communication (VLC), Light-Emitting Diodes (LED), On-Off Keying (OOK), Equalisation, Solar Panel.**

I. INTRODUCTION

Energy and bandwidth concerns are becoming increasingly significant in the context of enabling the enormous connection of numerous smart devices with the emergence of the internet of things (IoT) and machine to machine (M2M) Communication. The impending radio frequency (RF) spectrum crunch has spurred scientists to explore alternatives to traditional RF communication. As a result, optical wireless communications (OWC) is being considered to complement the RF spectrum since it utilizes an electromagnetic spectrum that is entirely unregulated. The traditional photo receivers such as PIN diode, avalanche photodiode (APD) provide high speed communication, but at the same time, they are costly and energy consuming since they require external supply for their operation. Low-cost silicon solar cells are now widely available as a result of modern production processes. This has encouraged researchers to look into their use in sectors other than renewable energy. Solar cells may use electromagnetic radiation from lasers, light-emitting diodes (LEDs) and sunlight to create electrical energy. As shown in fig 1, solar panel can simultaneously harvest energy and provide communication.

Solar cell based receiver find their applications in IoT devices, M2M communication, vehicle to vehicle (V2V) communication, vehicle to infrastructure (V2I) communication etc. By exploiting the solar panel capabilities, the future electric vehicles equipped with the modern solar panel design as well as road side units road side solar panel assisted unit can unlock the potential of green vehicular communication.

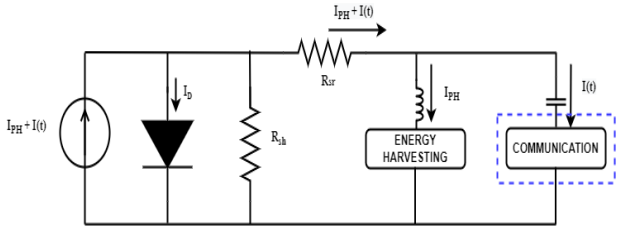

Fig. 1: Solar panel design for simultaneous energy harvesting and communication

Wireless communication using solar panel is a comparatively novel field of research. To understand the power consumption in VLC, paper [1] proposes a signal conditioning unit that will regularize the incoming signal deformed due to solar panel. The data rate of 8 kbit/s at a distance of 50 cm is achieved. The paper [2] addressed the pipe inspection application using VLC and solar panel as a receiver to increase the operation time of sensors. Reduction in peak-to-peak voltage from 3.9 V to 2.1 V at a distance of 1 m due to sunlight is observed. Bit error rate (BER) reported is 0.34% in water and 0.27% in air. In [3], solar panel is used to experimentally demonstrate an indoor positioning system. The optical power received at a distance of 2 m is $\sim$ 300 lux with a data rate of 2 kbps using OOK modulation scheme. The paper [4] proposes an architecture, which uses solar panel as a VLC receiver as well as for noise cancellation. According to test findings, ambient light noise genrated by indirect sunlight and other surrounding light sources can be reduced by using solar panel. The developed VLC system can operate at a frequency of 5.78 kHz and has a transmission distance of 40 cm. In [5], author demonstrated the solar panel feasibility of communication with OOK and orthogonal frequency division multiplexing (OFDM). At BER of 2×10^{-3}, the data rate of 1-Mbit/s was achieved at a distance of 39 cm. In an outdoor environment, VLC using solar panel works under the strong ambient light or sunlight. The author in [6] demonstrated that solar panel allows LiFi communications even at full sunlight exposure. In [7], the author demonstrated that under the strong

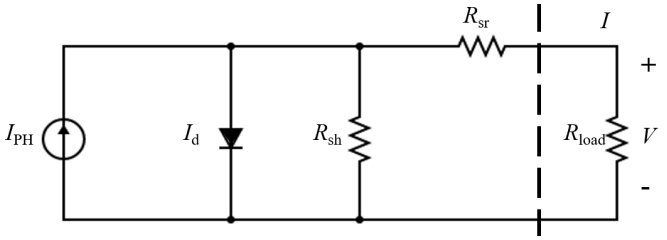

Fig. 2: Electrical equivalent model of solar panel

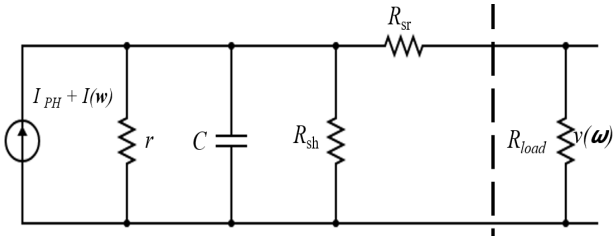

Fig. 3: AC model of solar panel

sunlight, their is slight drop in the signal strength and SNR when measured with respect to frequency. But at the same time the amount of energy harvested increase to the maximum power point level.

The present paper includes the reconfiguration of a receiver unit by using an bandwidth enhancement circuit (BEC) to enhance the 3 dB bandwidth substantially. A data rate of 1.5 Mbps is achieved at a distance of 1 m in the presence of ambient room light of 130 lux. A simple OOK modulation is used to achieve the reported data rate, in which the information is encoded in the form of logic low and logic high voltage levels. Testing with and without the BEC was done as part of the procedure, as well as for transmission demonstration. The rest of this paper is organized as follows. Section II describes the principle of operations of a solar panel, section III describes the bandwidth enhancement circuit design and its mathematical modeling. Communication capability in terms of various results is discussed in section IV followed by the concluding remarks in section V.

II. Principle of Operation of a Solar Panel

The DC model of solar panel is well studied in the past [8]-[9], the equivalent circuit model as shown in Fig. 2. Based on the solar panel responsivity, the generated electric current will flow through the internal diode and parasitic resistances. The current-voltage characteristics based on the single diode model is given by:

$$I = I_{PH} - I_d - \frac{V + I.R_{sr}}{R_{sh}} \tag{1}$$

$$V = I.R_{load} \tag{2}$$

$$I_d = I_0.exp\left[\frac{V + I.R_{sr}}{n.V_T} - 1\right] \tag{3}$$

In (1) shows that the relationship between current and voltage is nonlinear. The photocurrent source I_{PH} is connected in parallel with the diode, whose forward current is denoted as I_d. A series resistance R_{sr} depends on the interconnection among layers, and grid resistance [10]. The shunt resistance R_{sh} is due to the leakage current of the p-n junction. I_0 is the reverse saturation current of the diode, n is the number of cells in the series connection in a solar panel, and V_T thermal equivalent voltage of the diode.

To capture the AC characteristic of a solar panel the communication model needs to be followed as shown in Fig. 3. The main parameter of this AC model is the junction capacitor of the device, which corresponds to control the rise time and fall time of the incoming waveform. The capacitor C is placed in-parallel with the shunt resistance and the small-signal equivalent resistor r. When the light falls on the solar panel, current (I) gives the amount of photocurrent generated. This current consists of DC component as well as AC component, and by selecting proper filter values, the DC component of light can be blocked and only AC component will pass. The transfer function for the AC model is given by:

$$\left|\frac{V(w)}{I(w)}\right|^2 = \left|\frac{\frac{R_{load}}{(R_{load}+R_{sr})}}{1/r + jwC + 1/R_sh + 1/(R_{sr}+R_{load})}\right|^2 \tag{4}$$

where, ω is the angular frequency and $I(\omega)$ is the AC component of generated current.

For the OWC system the optical channel gain G, is given by:

$$G = \begin{cases} \dfrac{(m+1)A}{2\pi D^2}\cos^m(\phi)\cos(\psi) \\ \qquad\qquad 0 \le \psi \le \psi_c \ , \end{cases} \tag{5}$$

where, m denotes the order of Lambertian radiation pattern; D is the distance between transmitter and receiver; A is the physical area of the photo receiver; ϕ and ψ are the radiation and incidence angles, respectively.

III. Bandwidth Enhancement Circuit Design and Mathematical Modelling

For OOK modulated signal, the high-power level and low-power level of signal need to be differentiated at the receiver to extract the information within the signal. Because of the limited bandwidth of the solar panel receiver, the peak-to-peak level of the signal gets reduced and also the capacitive effect of solar panel affect the rise time and fall time of the incoming waveform, thus, distort the duty cycle of the incoming signal at higher switching frequency. Therefore, identification of logic high signal and logic low signal becomes difficult. To enhance the 3 dB bandwidth of the receiver system and improve the rise time and fall time of the incoming waveform, external circuitry needs to be incorporated in the solar panel receiver design, known as an equalizer.

This paper presents a BEC design for a solar panel as an OWC receiver as shown in Fig. 4. The overall receiver design consists of a solar panel, an equalizer, and a non-inverting amplifier. In this paper, the combination of an equalizer and non-inverting amplifier is considered as single unit called bandwidth enhancement circuitry. The BEC design is such that it filters out the DC component of received photocurrent at the

first stage and act on only AC component of the photocurrent. As the energy harvesting is predominantly consider the DC component of light, the BEC will not impact the energy harvesting of solar panel.

The mathematical analysis of the Fig. 4 is as follows:

$$\frac{V_1}{I} = \frac{\frac{R_1}{(R_1+R_{sr})}}{1/r + jwC + 1/R_{sh} + 1/(R_{sr}+R_1)} \tag{6}$$

$$\frac{V_2}{V_1} = \frac{R_2}{R_2 + (1/sC_2)} \tag{7}$$

As the circuit is having negative feedback, from virtual ground concept: $V_2 = V_3$

$$\frac{V_4}{V_3} = 1 + \frac{R_3}{R_5} \tag{8}$$

$$\frac{V_5}{V_4} = \frac{R_4}{R_4 + R_8} \tag{9}$$

$$\frac{V_{out}}{V_5} = 1 + \frac{R_6}{R_7} \tag{10}$$

Here, $V_{out} = v(w)$

from equation (9), equation (10) and from virtual ground concept ($V_5 = V_6$)

$$\frac{V_{out}}{V_4} = \left(\frac{R_4}{R_4 + R_8}\right).\left(1 + \frac{R_6}{R_7}\right) \tag{11}$$

from equation (7), equation (8) and equation (11)

$$\frac{V_{out}}{V_1} = \left(\frac{R_4}{R_4 + R_8}\right).\left(1+\frac{R_3}{R_5}\right).\left(1+\frac{R_6}{R_7}\right).\left(\frac{R_2}{R_2 + (1/sC_2)}\right) \tag{12}$$

from equation (6) and equation (11)

$$\frac{V_{out}}{I} = \left(\frac{\frac{R_1}{(R_1+R_{sr})}}{1/r + jwC + 1/R_{sh} + 1/(R_{sr}+R_1)}\right).$$

$$\left(\frac{R_4}{R_4 + R_8}\right).\left(1 + \frac{R_3}{R_5}\right).\left(1 + \frac{R_6}{R_7}\right).\left(\frac{R_2}{R_2 + (1/sC_2)}\right) \tag{13}$$

The modified receiver transfer function is given in (13). The overall system response includes the solar panel response in cascade with the response of BEC. The frequency response and the time response of the designed receiver are described in the results section.

IV. Experiment setup

A 5-watts polycrystalline solar panel is used for experiment and the solar panel parameter values are given in Table I. To evaluate the performance of a solar panel receiver with and without BEC, testing is performed with the setup block diagram as given in Fig. 5. It consists of arbitrary waveform generator (AWG), LED driver circuit, 24 LED's panel, 5 W solar panel, BEC and an oscilloscope. The testing is done in the presence of room light of 130 lux. A 5 W solar panel with 18 cells arranged in a 9×2 configuration is used. The other parameters are given in table II. The testing setup is given in Fig. 6, where the transmission distance is of 1 m. The receiver unit comprises of solar panel, BEC, digital signal processing board to process the incoming data, and a laptop.

TABLE I: Solar panel parameters

Parameters	Parameter Values
Number of cells	18 (9×2)
Open circuit voltage (V_{oc})	11.24 V
Short Circuit Current (I_{sc})	0.64 A
Rated Voltage (V_{mp})	9.23 V
Rated Current (I_{mp})	0.56 A
Module efficiency (η)	8.55 %

TABLE II: Testing Parameters

Parameters	Parameter Values
Number of LEDs	24
Electrical power	14.4 W
Distance	1 m
Average optical irradiance at solar panel	1800 Lux
Ambient light at solar panel	130 Lux
Solar panel	5 W (18 Cells)

Fig. 7 shows V-I characteristics of 5 W solar panel under standard testing conditions. V-I characteristics plays an important role in estimation of DC parameter of solar panel [11]–[13]. Series resistance and shunt resistance value for the considered solar panels are 0.88 Ω and 225.54 Ω respectively. The minimum and the maximum values of series resistance and shunt resistance for known values of solar panel parameter [14] [15] are given by:

$$R_{s;min} = 0 \tag{14}$$

$$R_{s;max} = \frac{V_{oc} - V_{mp}}{I_{mp}} \tag{15}$$

Using [16] the parasitic resistance are calculated. By using the slopes of the I-V characteristic at the short circuit and open circuit points, the initial values of resistance can be obtained:

$$R_{s0} = -\left(\frac{\partial V}{\partial I}\right)\Bigg|_{V=V_{OC}} \tag{16}$$

$$R_{sh0} = \left(\frac{\partial V}{\partial I}\right)\Bigg|_{I=I_{SC}} \tag{17}$$

once the initial values are verified within the range specified in (14)-(15), the values can be further optimized in terms of known parameter values as follows:

$$R_s = \frac{(A-B)V_{mp}}{(A+B)V_{mp}} + \frac{B}{(A+B)}\frac{V_{oc}}{I_{mp}} \tag{18}$$

Where,

$$A = (V_{mp}+(I_{mp}-I_{SC})R_{sh0})ln\left(\frac{V_{mp} + (I_{mp} - I_{SC})R_{sh0}}{V_{oc} - I_{SC}R_{sh0}}\right) \tag{19}$$

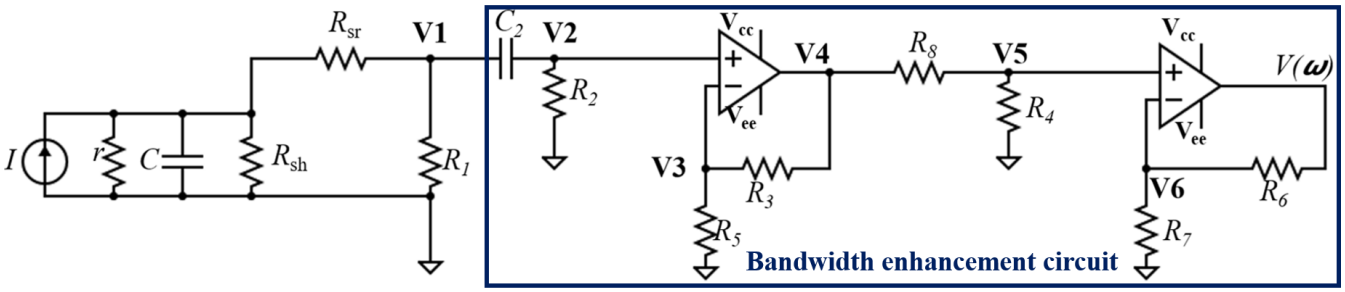

Fig. 4: Solar panel receiver

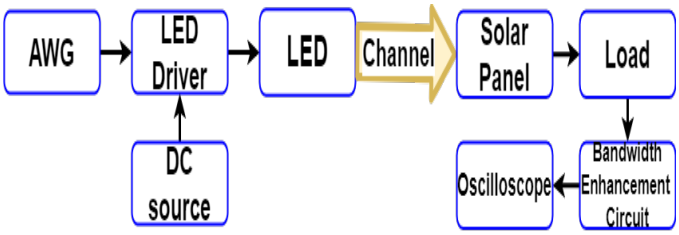

Fig. 5: Block diagram of communication setup

Fig. 6: Testing setup

and

$$B = V_{mp} - R_{sh0} I_{mp} \tag{20}$$

$$R_{sh} = R_{sh0} \tag{21}$$

The obtained values are utilized to reconstruct the I-V curve using Newton-Raphson iterative method [17].

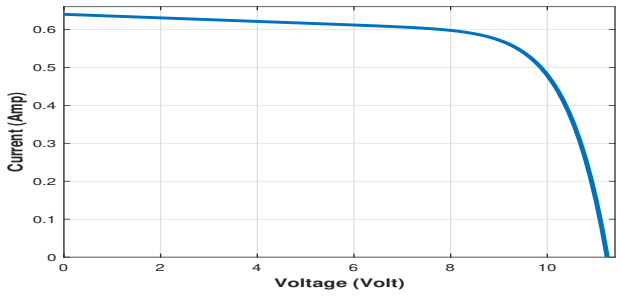

Fig. 7: V-I Characteristic of solar panel

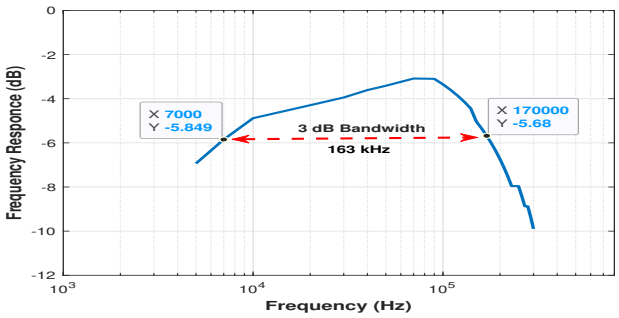

Fig. 8: Frequency response of solar panel

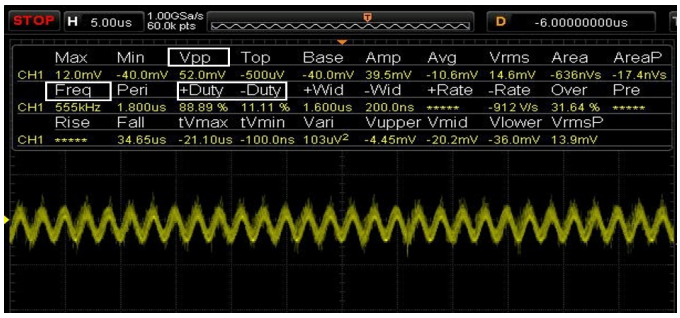

Fig. 9: Solar panel time response

V. Results and Discussion

The solar panels are basically designed to maximize the energy harvesting [18]–[20], and their bandwidth is in the range of few kHz. The tested solar panel is having 3 dB bandwidth of 163 kHz as shown in Fig. 8. The maximum operation region with solar panel is upto 400 kHz as thereafter the peak to peak voltage level is very low and duty cycle of the received waveform is uneven as shown in Fig. 9. As solar panel also passes the DC component of light, solar panel output consist of DC signal along with the time varying signal. Presence of DC signal will saturate the output, thereby decision making for logic low and logic high will become complicated. To retrieve the transmit data at receiver, the minimum peak to peak voltage level need to be maintained, that results in a decision for logic high or logic low sample values. Therefore, for the communication purpose the DC signal needs to be blocked. To block the DC signal and improve the 3 dB receiver

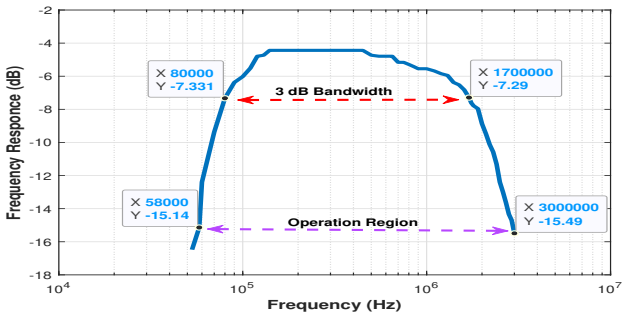

Fig. 10: Frequency response of modified receiver design

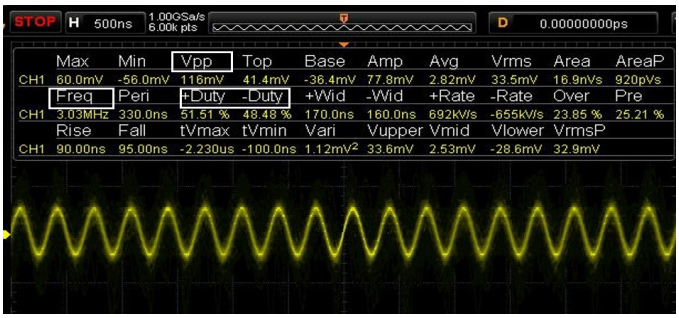

Fig. 11: Time response of modified receiver

bandwidth an bandwidth enhancement circuit stage is used. A bandwidth enhancement circuit stage after the solar panel in receiver circuit increased the 3 dB bandwidth to 1.62 MHz as shown in Fig. 10. As the 3 dB bandwidth of the receiver is increased, the switching frequency up to which information can be extracted is also increased. With the help of BEC, the peak-to-peak voltage level is maintained high enough to distinguish between logic low and logic high level at 3 MHz. The duty cycle of the received signal is also improved, as shown in Fig. 11. The conversion of generated current into voltage is done with the help of resistor R_1 instead of a trans-impedance amplifier (TIA). A trans-impedance amplifier is not a suitable solution in this case, as solar panel generate more DC because of larger sensing area of solar panel and most of the op-amps necessary to design a trans-impedance amplifier will get saturated. It will not work specifically in outdoor scenario where sunlight comes in play, generating high DC at solar panel hence will saturate op-amps. It is more practical to first do current to voltage conversion using passive component and then separate DC and AC and use AC part of signal for communication. The load resistor before the BEC play an crucial role in deciding the input voltage signal for the BEC. The low value of load resistor will result in higher bandwidth but the signal peak- to-peak is very low and BEC will not be able to process the incoming signal, whereas higher value of load resistor may saturate the signal value which will result into clipping of the incoming signal. Therefore, selection of load resistor along with the BEC parameter values place an crucial role to decide the receiver response. BEC signal is fed to ADC for further processing and a low pass filter is integrated at the input of ADC to block the higher frequency noise. The eye diagram at 1.5 Mbps of data rate is shown in

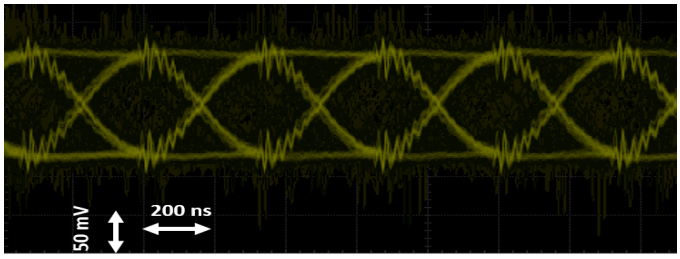

Fig. 12: Eye pattern at the data rate of 1.5 Mbps

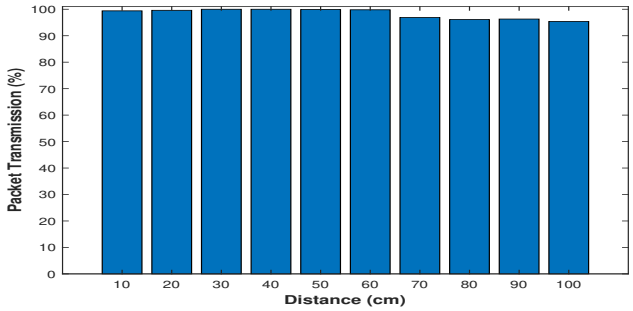

Fig. 13: Packet success rate during transmission with distance

Fig. 12. The effect of distance between transmitter and receiver on successful transmission of packet is shown in Fig. 13. The testing was carried out by transmitting 1000 packets with each packet having 1518 bytes of length and it is observed that packet loss increases after 100 cm. The reason of increase in packet loss includes the divergence of light and responsivity of each solar cell. With distance light will diverge and hence the amount of light collected by each cell will decrease. At the receiver the analog circuit will not be able to produce the required peak-to-peak level and thus the decision making become difficult for analog to digital convertor. It may also be noted that at shorter distance (less than 30 cm), light source is very close to solar panel therefore, only few cells are getting illuminated resulting in slight degradation in performance.

Fig. 14 shows the impact of transmission distance on the data rate for range of transmitted power. When the light source moves towards the solar panel, the maximum data rate is achieved at lower value of transmitted power as the optical power required to attain the desired extinction ratio is obtained. The trend can be observed in all the distance measurements. It may also be noted that at a distance of 40 cm, the light source is very close to solar panel and therefore, cells are getting high intensity of light. The maximum data rate is achieved at 6 W of power. When the power increases beyond 7 W the amount of peak-to-peak voltage received by the amplifying unit is beyond the linear region. Thus, clipping of the signal occurs due to reduction in peak to peak voltage, thereby leading to data loss. As the power level keeps on increasing, the data rate will decay and it saturates to 850 kbps beyond the power level of 11.5 W.

VI. Conclusion

This paper proposed a receiver for optical wireless communication using solar panel as a receiver. Experimental results

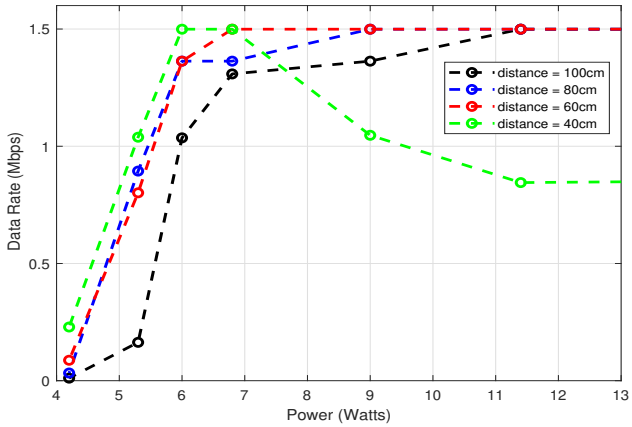

Fig. 14: Data rate Vs power

shows that by utilizing the external circuitry along with the solar panel, an enhanced bandwidth can be achieved. A VLC link of 1 m is presented on which the data rate of 1.5 Mbps is achieved with OOK modulation. According to best of our knowledge, this is the highest reported data rate with the distance of 1 m using white light in an indoor scenario with OOK modulation. The experiments are performed under the room light of 130 lux. The enhanced bandwidth of the receiver shows that with the multi-carrier modulation schemes, higher data rate can be achieved by doing minimal changes in the circuit design. For future work energy harvesting through solar panel can also be done. As the present experiment is performed in the indoor environment the amount of energy harvested using VLC transmitter is 15 mW. However the harvested power is less but it will supplement a portion of electrical power required to operate the BEC circuitry. In an outdoor environment solar panel can harvest power upto its respective maximum power point. Thereby, harvested energy in outdoor can be utilized to supply a larger portion of 0.24 W of electrical power required to operate the BEC.

VII. Acknowledgement

This publication is an outcome of the research and development work undertaken project of Ministry of Electronics Information Technology, Government of India.

Rahul would like to thank University Grant Commission (UGC) for awarding fellowship under junior research fellowship, Department of Higher Education, Ministry of Education, Government of India. We would like to acknowledge Abhijit Mitra for this work who is supported by a DST Inspire Faculty Award (DST/INSPIRE/04/2017/000089).

References

[1] B. Malik and X. Zhang, "Solar panel receiver system implementation for visible light communication," in *2015 IEEE International Conference on Electronics, Circuits, and Systems (ICECS)*. Cairo: IEEE, Dec. 2015, pp. 502–503.

[2] W. Zhao, M. Kamezaki, K. Yamaguchi, M. Konno, A. Onuki, and S. Sugano, "An Experimental Analysis of Pipe Inspection using Solar Panel Receiver for Visible Light Communication and Energy Harvesting," in *2020 IEEE/ASME International Conference on Advanced Intelligent Mechatronics (AIM)*. Boston, MA, USA: IEEE, Jul. 2020, pp. 1848–1853.

[3] C.-W. Hsu, J.-T. Wu, H.-Y. Wang, C.-W. Chow, C.-H. Lee, M.-T. Chu, and C.-H. Yeh, "Visible Light Positioning and Lighting Based on Identity Positioning and RF Carrier Allocation Technique Using a Solar Cell Receiver," *IEEE Photonics Journal*, vol. 8, no. 4, pp. 1–7, Aug. 2016.

[4] K. Sindhubala and B. Vijayalakshmi, "Receiver Intend to Reduce Ambient Light Noise in Visible - Light Communication using Solar Panels," *Journal of Engineering Science and Technology Review*, vol. 10, no. 1, pp. 84–90, Feb. 2017.

[5] Z. Wang, D. Tsonev, S. Videv, and H. Haas, "Towards self-powered solar panel receiver for optical wireless communication," in *2014 IEEE International Conference on Communications (ICC)*. Sydney, NSW: IEEE, Jun. 2014, pp. 3348–3353.

[6] N. Lorriere, J.-J. Simon, N. Betrancourt, M. Pasquinelli, G. Chabriel, J. Barrere, L. Escoubas, J.-L. Wu, V. Bermudez, and C. Ruiz, "Photovoltaic Solar Cells for Outdoor LiFi Communications," *Journal of Lightwave Technology*, pp. 1–1, 2020.

[7] S. Das, A. Sparks, E. Poves, S. Videv, J. Fakidis, and H. Haas, "Effect of Sunlight on Photovoltaics as Optical Wireless Communication Receivers," *Journal of Lightwave Technology*, vol. 39, no. 19, pp. 6182–6190, Oct. 2021.

[8] S. Bader, X. Ma, and B. Oelmann, "One-diode photovoltaic model parameters at indoor illumination levels – A comparison," *Solar Energy*, vol. 180, pp. 707–716, Mar. 2019.

[9] D. Sera, R. Teodorescu, and P. Rodriguez, "PV panel model based on datasheet values," in *2007 IEEE International Symposium on Industrial Electronics*. Vigo, Spain: IEEE, Jun. 2007, pp. 2392–2396.

[10] F. Lasnier and T. Ang, "Book chapter,chapter 6: Power conditioning systems," *Adam Hilger, Bristol and New York, Photovoltaic Engineering Handbook*, 1990.

[11] K. Bouzidi, M. Chegaar, and A. Bouhemadou, "Solar cells parameters evaluation considering the series and shunt resistance," *Solar Energy Materials and Solar Cells*, vol. 91, no. 18, pp. 1647–1651, Nov. 2007.

[12] M. Villalva, J. Gazoli, and E. Filho, "Comprehensive Approach to Modeling and Simulation of Photovoltaic Arrays," *IEEE Transactions on Power Electronics*, vol. 24, no. 5, pp. 1198–1208, May 2009.

[13] M. Diantoro, T. Suprayogi, A. Hidayat, A. Taufiq, A. Fuad, and R. Suryana, "Shockley's Equation Fit Analyses for Solar Cell Parameters from I-V Curves," *International Journal of Photoenergy*, vol. 2018, pp. 1–7, 2018.

[14] H. A. B. Siddique, P. Xu, and R. W. De Doncker, "Parameter extraction algorithm for one-diode model of PV panels based on datasheet values," in *2013 International Conference on Clean Electrical Power (ICCEP)*. Alghero, Italy: IEEE, Jun. 2013, pp. 7–13.

[15] J.-Y. Park and S.-J. Choi, "A novel datasheet-based parameter extraction method for a single-diode photovoltaic array model," *Solar Energy*, vol. 122, pp. 1235–1244, Dec. 2015.

[16] J. Cubas, S. Pindado, and M. Victoria, "On the analytical approach for modeling photovoltaic systems behavior," *Journal of Power Sources*, vol. 247, pp. 467–474, Feb. 2014.

[17] M. S. Hossain, N. K. Roy, and M. O. Ali, "Modeling of solar photovoltaic system using MATLAB/Simulink," in *2016 19th International Conference on Computer and Information Technology (ICCIT)*. Dhaka, Bangladesh: IEEE, Dec. 2016, pp. 128–133.

[18] M. Kong, C. H. Kang, O. Alkhazragi, X. Sun, Y. Guo, M. Sait, J. A. Holguin-Lerma, T. K. Ng, and B. S. Ooi, "Survey of energy-autonomous solar cell receivers for satellite–air–ground–ocean optical wireless communication," *Progress in Quantum Electronics*, vol. 74, p. 100300, Nov. 2020.

[19] R. R. King, D. Bhusari, D. Larrabee, X.-Q. Liu, E. Rehder, K. Edmondson, H. Cotal, R. K. Jones, J. H. Ermer, C. M. Fetzer, D. C. Law, and N. H. Karam, "Solar cell generations over 40% efficiency: Solar cell generations over 40% efficiency," *Progress in Photovoltaics: Research and Applications*, vol. 20, no. 6, pp. 801–815, Sep. 2012.

[20] M. A. Green, K. Emery, Y. Hishikawa, W. Warta, and E. D. Dunlop, "Solar cell efficiency tables (Version 45): Solar cell efficiency tables," *Progress in Photovoltaics: Research and Applications*, vol. 23, no. 1, pp. 1–9, Jan. 2015.